Pressure-induced structural phase transition in NaBH$_4$

C. Moysés Araújo,[1] R. Ahuja,[1] A. V. Talyzin,[2] and B. Sundqvist[2]

[1]*Condensed Matter Theory Group, Department of Physics, Uppsala University, Box 530, SE-751 21 Uppsala, Sweden*
[2]*Department of Physics, Umeå University, S-901 87 Umeå, Sweden*

We present a combined experimental and theoretical study of the technologically important NaBH$_4$ compound under high pressure. Using Raman spectroscopy at room temperature, we have found that NaBH$_4$ undergoes a structural phase transformation starting at 10.0 GPa with the pure high-pressure phase being established above 15.0 GPa. In order to compare the Raman data recorded under high pressure with the low-temperature tetragonal phase of NaBH$_4$, we have also performed a cooling experiment. The known order-disorder transition from the fcc to the tetragonal structure was then observed. However, the new high pressure phase does not correspond to this low-temperature structure. Using first-principle calculations based on the density functional theory, we show that the high-pressure phase corresponds to the α-LiAlH$_4$–type structure. We have found a good agreement between the measured and calculated transition pressures. Additionally, we present the electronic structure of both the fcc and the high-pressure phases.

PACS number(s): 64.70.Kb, 61.50.Ks, 71.15.Mb

I. INTRODUCTION

The complex alkali hydrides (MXH$_4$ with $M=$ Na, Li and $X=$ Al, B) have attracted considerable attention, mainly for being promising hydrogen storage materials due to their high hydrogen content (up to 18.4 wt. % in LiBH$_4$).[1,2] However, in these systems the hydrogen is held by strong covalent and ionic bonds resulting in high dissociation temperatures. These features limit their practical applications to hydrogen storage. To overcome such limitations, a great deal of research has been conducted to study the role of catalytic agents on their thermodynamic properties, which is motivated by the discovery that addition of a Ti-based catalyst in NaAlH$_4$ can significantly lower the hydrogen desorption temperature.[3] In addition to these attempts to make the complex alkali hydrides more suitable as hydrogen storage materials, much effort has also been paid to understand their behavior under high pressure.[4–6] These compounds are expected to undergo several structural phase transformations displaying novel characteristics. For instance, it was recently predicted theoretically[5] and verified experimentally[6] that LiAlH$_4$ undergoes a phase transition at 2.6 GPa. Theory predicted a huge volume collapse of 17%, which would significantly increase its hydrogen packing density. In this area, first-principles calculations have not only been shown to be reliable but have actually played an important role, since it is very difficult to determine the hydrogen positions by high-pressure diffraction techniques.

Recently, NaBH$_4$ slurry was suggested as a promising system for applications in fuel cell technology.[7–10] It is a very efficient storage system (9.2 wt. %), and also provides a simple way for generating hydrogen through the exothermal reaction NaBH$_4+2$H$_2$O$\rightarrow$NaBO$_2+4$H$_2$. This reaction is activated by adding a proper catalyst agent and can operate at ambient conditions. Furthermore, the by-product NaBO$_2$ can be recycled into NaBH$_4$ through a fuel recovery reaction that makes the hydrolysis above a reversible process.[8] Additionally, NaBH$_4$ itself is also a promising hydrogen storage material since it has one of the highest gravimetric hydrogen densities (10.5 wt. %) among the alkali metal hydrides.[1] Despite such recognized technological importance only little is known about its fundamental physical properties. Furthermore, no high pressure study has been reported yet.

In this work, we present a combined experimental and theoretical study of NaBH$_4$ under high pressure. Using Raman spectroscopy, we show that NaBH$_4$ undergoes a structural phase transformation starting at 10.0 GPa with the pure high-pressure phase being established above 15.0 GPa. This transition is shown to be reversible on pressure release. From the analysis of the Raman spectra, the high pressure phase is suggested to be either orthorhombiclike or monocliniclike with the BH$_4$ cluster displaying lower symmetry. In order to compare the Raman data recorded under high pressure with the possible low-temperature tetragonal phase of NaBH$_4$, we have also performed a cooling experiment. The known order-disorder transition from the fcc to the tetragonal structure was then observed. However, the new high-pressure phase does not correspond to this low-temperature structure. Using *ab initio* theoretical methods we have studied six closely related potential structures. They are namely tetragonal-$P$$-42_1c$ (low-temperature phase), α-NaBH$_4$ (cubic-$F43m$), α-LiAlH$_4$ (monoclinic, $P2_1/c$), α-NaAlH$_4$ (tetragonal-$I4_1/a$), KGaH$_4$ (orthorhombic-$Cmc2_1$), α-LiBH$_4$ (orthorhombic-$Pnma$). We show that the high-pressure phase corresponds to the α-LiAlH$_4$ type structure. The calculated transition pressure of 19.0 GPa agrees quite well with the experimental value of 15.0 GPa. A subsequent phase transition from α-LiAlH$_4$– to α-LiBH$_4$–type structure is expected to occur at 33.0 GPa. In addition, we discuss the electronic structure of both the α-NaBH$_4$ and the high-pressure phase.

II. EXPERIMENTAL AND COMPUTATIONAL METHODS

NaBH$_4$ of 97% purity was purchased from Merck and studied using a diamond-anvil cell (DAC) with 0.4-mm flat culets. Using an argon-filled glove box the sample was loaded into a 0.2-mm hole in the DAC steel gasket together with a ruby chip used for pressure calibration, without any pressure-transmitting medium. The accuracy of the pressure

measurements is estimated as ±0.5 GPa. An x-ray diffraction (XRD) test of the starting material confirmed good structural quality. Only peaks due to the $NaBH_4$ fcc structure were observed and the calculated cell parameter $a=6.16$ Å is in good agreement with literature data.[11] A Renishaw Raman 1000 spectrometer with a 514 nm excitation laser and a resolution of 2 cm^{-1} was used in these experiments. Raman spectra were recorded *in situ* through the diamond anvils using a long focus 20$^\times$ objective during both compression and decompression, using pressure steps of 1–1.5 GPa. Spectra for the starting material and for the sample loaded into the DAC were identical. The pressure was increased gradually with Raman spectra recorded on every step during compression and decompression. Usually, the total time spent at each pressure step was 1–2 h. For the low-temperature measurements a Linkam FDCS 196 cold stage cryogenic cell cooled by cold nitrogen gas was used. Again, samples were loaded into the cell under Ar gas in a glovebox with sub-ppm levels of H_2O and O_2.

The electronic structure and the total energy were calculated within the framework of the generalized gradient approximation (GGA) to density functional theory (DFT) (Ref. 12) using projected augmented wave (PAW) (Ref. 13) method as implemented in the VASP code.[14] We have used the exchange-correlation potential of Perdew *et al.*[15] The PAW potentials with the valence states $2p$ and $3s$ for Na, $3s$ and $3p$ for B, and $1s$ for H were used. For sampling the irreducible wedge of the Brillouin zone we used k-point grids of $7\times7\times7$ for the geometry optimization and $9\times9\times9$ for the final calculation at the equilibrium volume, which were generated according to the Monkhost-Pack scheme. The relaxations of the structures were performed by using the conjugated-gradient algorithm[16] and by considering the minimization of both the forces and stress tensors. In all calculations, self-consistency was achieved with a tolerance in the total-energy of at least 0.1 meV/atom. The density of states (DOS) for static configurations was calculated by means of the modified tetrahedron method of Blöchl *et al.*[17]

The equilibrium volume (V_0), bulk modulus (B_0) at ambient pressure and its first derivative (B_0') were estimated through a least-square fit of calculated total energy- (E-) volume (V) set to the Murnaghan equation of states. The hydrostatic pressure as a function of the volume were calculated from the first derivative of the $E-V$ curve using the obtained values for V_0, B_0, and $2B_0'$, whereas the transition pressure is determined by evaluating the enthalpy ($E+PV$, at $T=0$) for the two different phases. At a given pressure, the stable structure is the one that has the lowest enthalpy.

III. RESULTS AND DISCUSSIONS

Raman spectra of $NaBH_4$ at normal conditions exhibit mostly internal modes of the $[BH_4]^-$ ionic clusters. In the region of B-H stretching vibrations (2100–2500 cm^{-1}) the spectrum is dominated by the symmetric stretching mode ν_1 at 2332 cm^{-1}. The bending modes ν_2 (1121 cm^{-1}) and ν_4 (1277 cm^{-1}) are relatively weak, and these modes were impossible to observe in our DAC experiments since they were too close to the diamond peak from the anvils. How-
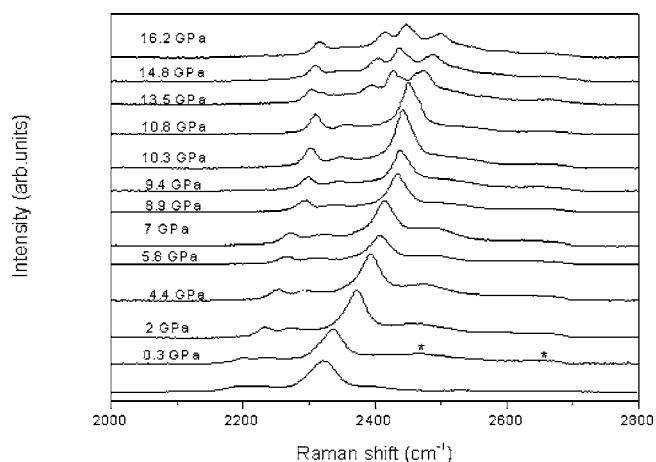

FIG. 1. Raman spectra of $NaBH_4$ recorded during the compression part of experiment. Broad peaks from diamond anvil impurities are marked with asterisks on the spectrum obtained at 0.3 GPa. A spectrum of the original $NaBH_4$ recorded outside the DAC is shown for comparison (bottom).

ever, the combination band $\nu_2+\nu_4$ and the overtones $2\nu_4(A_1)$ and $2\nu_4(F_2)$ are reasonably strong and can usually be observed close to ν_1. Unfortunately, specific defects/impurities in our diamonds also resulted in broad Raman peaks above 2400 cm^{-1}. As a result of this unfortunate coincidence only the evolution of the main peaks ν_1, $2\nu_4(A_1)$, and $2\nu_4(F_2)$ could be studied as a function of pressure. Figure 1 shows the pressure dependence of the Raman spectrum of $NaBH_4$ in the pressure region up to 16.2 GPa recorded during compression. Peaks originating from the diamonds are indicated by asterisks in the spectrum recorded at 0.3 GPa. Analysis of Fig. 1 shows that $NaBH_4$ clearly undergoes a phase transition above 10.0 GPa. Peaks from a new phase can be recognized already in the spectrum recorded at 10.8 GPa, at 13.5 GPa peaks from both low-pressure and high-pressure modifications can be seen simultaneously and finally at 14.8 GPa only peaks from the new high pressure phase can be observed. At the highest pressure achieved in this experiment (16.2 GPa), peaks of the new phase are situated at 2315, 2413, 2449, and 2500 cm^{-1}.

The evolution of the peak positions during compression is shown in Fig. 2. The positions shift almost linearly with pressure above 2.0 GPa. Such a linear shift, but with a different slope, is also observed in the pressure region 0-2 GPa where only three individual points were measured. The exact nature of the observed change in slope is not clear, but we speculate that it might be connected with the ordering transition observed at low temperature or freezing of local molecular motion. We also note from Fig. 1 that the relative intensities of some peaks are changed near 2.0 GPa.

The sample was held for several days at maximum pressure without detection of any changes in the Raman spectrum. The decompression part of the experiment is shown in Figs 3 and 4. As can be seen from these figures, the phase transition is reversible and the high-pressure modification reverts back to normal α-$NaBH_4$ during pressure release. The phase transition from the high-pressure phase to the low-pressure phase can be observed to start at 10.8 GPa. At 8.3
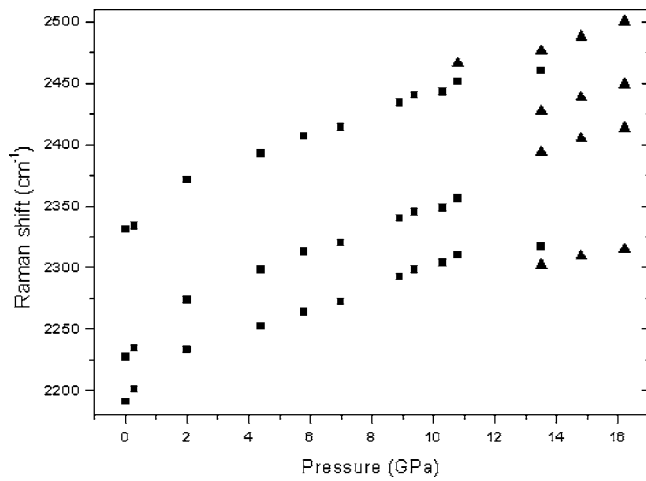
FIG. 2. Peak positions found in the Raman spectra of NaBH$_4$ on compression. A phase transition occurs in the interval 12.8–14.8 GPa. Peaks from the high-pressure phase are indicated by triangles.

FIG. 4. Peak positions of the Raman spectra of NaBH$_4$ on decompression.

GPa we observe peaks from both phases and at 7.0 GPa only peaks from the low-pressure phase can be observed.

The structure of the high-pressure phase found to exist above 10–15 GPa could not be determined from our Raman data. Only a few main peaks could be followed in our experiments due to the unfortunate coincidence of some peak positions from NaBH$_4$ with DAC-related Raman peaks. Nevertheless, it can be concluded from our data that the symmetry of the BH$_4$ ionic cluster is reduced in the high pressure phase. Instead of the single strong peak ν_1 due to symmetric B-H stretching in α-NaBH$_4$ the high-pressure phase exhibits three similarly strong peaks in the same region. Such a spectrum can be consistent with, for example, an orthorhombic structure (as in LiBH$_4$, for example) or a monoclinic one.

In principle, the new phase could be identical to the known low-temperature tetragonal phase of NaBH$_4$.[18] The phase transition between the tetragonal and fcc structures is of first order and occurs at ~186–190 K.[19] According to NMR data this phase transition is due to an order-disorder transformation,[20] and it is also interesting to note that the two
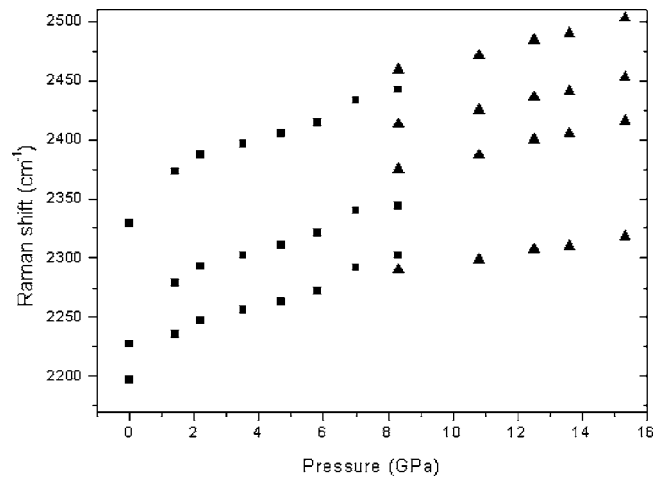
phases were observed to coexist in a narrow temperature interval. This phase transition is relatively little studied and Raman spectra for the low-temperature phase have been published only for NaBD$_4$. Order-disorder phase transitions, which occur at low temperatures, are often observed at room temperature upon pressure increase, and one well-studied example of such a phase transformation is the orientational ordering transition in C$_{60}$.[21]

In order to compare Raman spectra of the low-temperature tetragonal phase of NaBH$_4$ with our high-pressure data a cooling experiment was performed. Raman spectra recorded upon cooling are shown in Fig. 5 and the evolution of the peak positions is shown in Fig 6. As can be seen in Fig. 5 the phase transition from fcc to the low temperature tetragonal phase occurs in the temperature range 193–183 K. Additional peaks and a significant sharpening of the original Raman peaks are observed below the transition temperature, in good agreement with the known order-disorder nature of this transformation.[20] If we compare the Raman spectra of the tetragonal phase with the spectra recorded at high pressure conditions, it is clear that the new
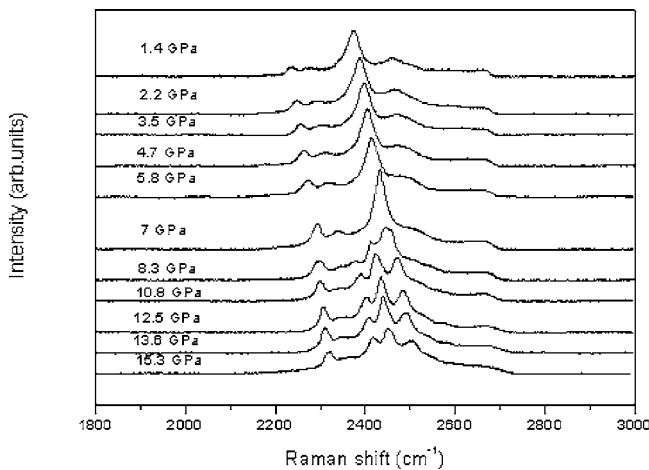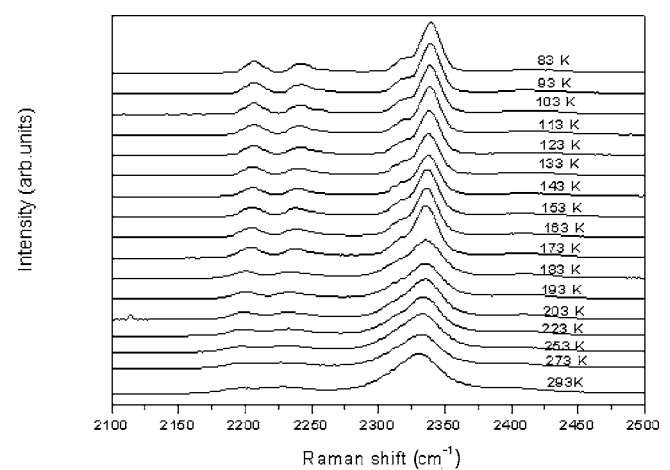

FIG. 3. Raman spectra recorded on decompression of NaBH$_4$.

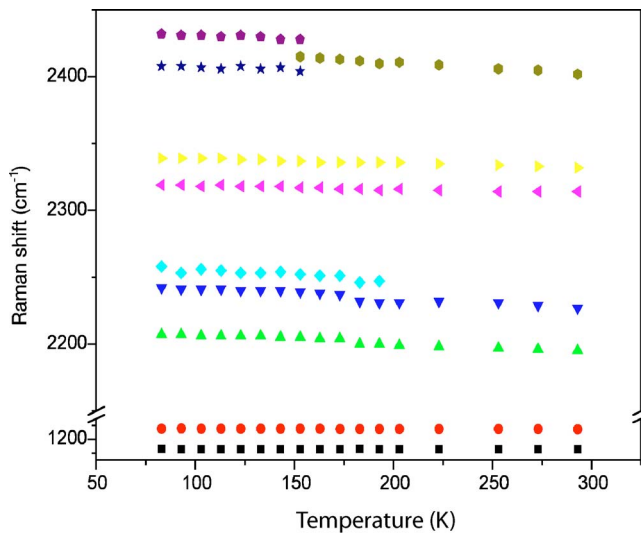FIG. 5. Raman spectra of NaBH$_4$ recorded upon a cooling from 293 down to 83 K.

FIG. 6. (Color online) Temperature dependence of the Raman modes of NaBH$_4$.

FIG. 7. The energy-volume relation for all structures considered in the calculation.

high pressure phase observed in our experiments above 11 GPa is very different from tetragonal NaBH$_4$.

Our first-principles total energy calculations were performed at zero temperature. We have therefore found that the NaBH$_4$ ground-state corresponds to the tetragonal (P -42_1c) phase in good agreement with the experimental findings for the low-temperature structure. Furthermore, we have found that this structure remains stable in whole pressure range considered in this work. It means that no pressure-induced phase transition is expected to occur at low temperature.

Since high-pressure experiments are performed at room temperature, we have taken the experimentally observed room temperature phase namely fcc phase as ground state to compare it with four other closely related phases. In Fig. 7, we show the calculated cohesive energy as a function of the volume for all possible phases, except for KGaH$_4$ type (orthorhombic-$Cmc2_1$) phase that has shown to be much less stable than the others. As can be seen from Fig. 7, the fcc (α-NaBH$_4$) structure is stable at ambient pressure and at 19 GPa it shows a transition to the α-LiAlH$_4$–type structure (β-NaBH$_4$ phase). A subsequent transformation occurs from the β-NaBH$_4$ to the α-LiBH$_4$ type structure (γ-NaBH$_4$ phase) at 33 GPa. In order to show more clearly these transitions, we display, in Fig. 8, the enthalpy difference for the β and γ phases as well as for the NaAlH$_4$-type phase as a function of pressure with reference to α-NaBH$_4$. In our *ab initio* calculations, we cannot treat the coexisting phases. Thus, all calculated transitions are for the pure phases. We should therefore compare the theoretical value of 19 GPa with the experimental finding of 15 GPa, which are in good agreement. Furthermore, in the α-LiAlH$_4$–type structure the nearest B-H bond lengths vary between 1.22 and 1.23 Å, yielding a slightly distorted tetrahedral configuration. Such a deformation agrees with the experimental observation that the symmetry of BH$_4$ ionic cluster is reduced at high pressure.

The total DOS for the α-NaBH$_4$ phase at ambient pressure is presented in Fig. 9(a). It displays an insulator behav-
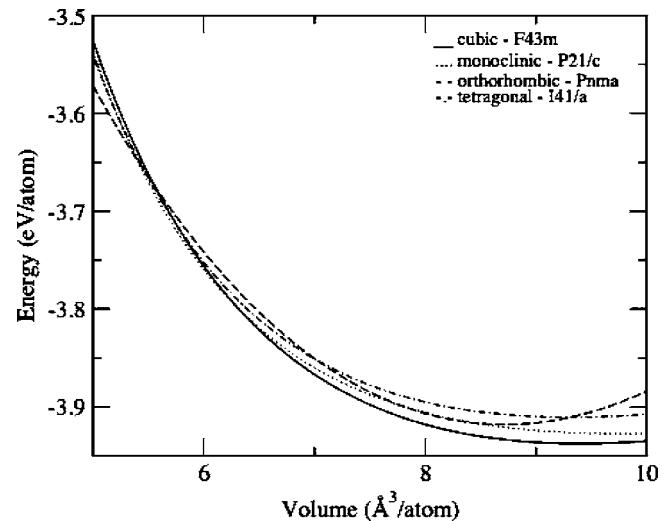
ior characterized by a band gap of nearly 6.5 eV, which is quite close to the recent theoretical value of 6.2 eV for LiBH$_4$.[22] The valence band is split into two regions. The low-energy band is composed of B 2s and H 1s states with a bandwidth of 1.33 eV, whereas, the high-energy band is composed mainly by hybridization between H 1s and B 2p states with a bandwidth of 2.08 eV. These are consistent with the directional covalent bond that occurs between the boron and hydrogen atoms. The bottom of the conduction band just above the Fermi energy is composed primarily by the Na p and s antibonding states which is consistent with the ionic bonding between the Na and the BH$_4$ unit. In Fig. 9(b), we present the total DOS for the β-NaBH$_4$. The main features are very similar to those described above for α-NaBH$_4$. The main difference is a narrower band gap of 6.3 eV. The origin of this reduction is found to be due to the broadening of the Na antibonding states in the conduction band, which is asso-
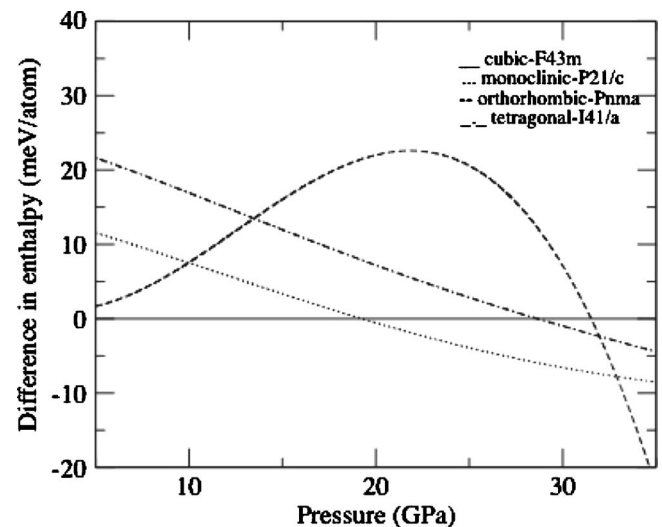

FIG. 8. The difference in enthalpy for LiAlH$_4$, LiBH$_4$, and NaAlH$_4$ type structures with reference to α-NaBH$_4$ as a function of pressure.
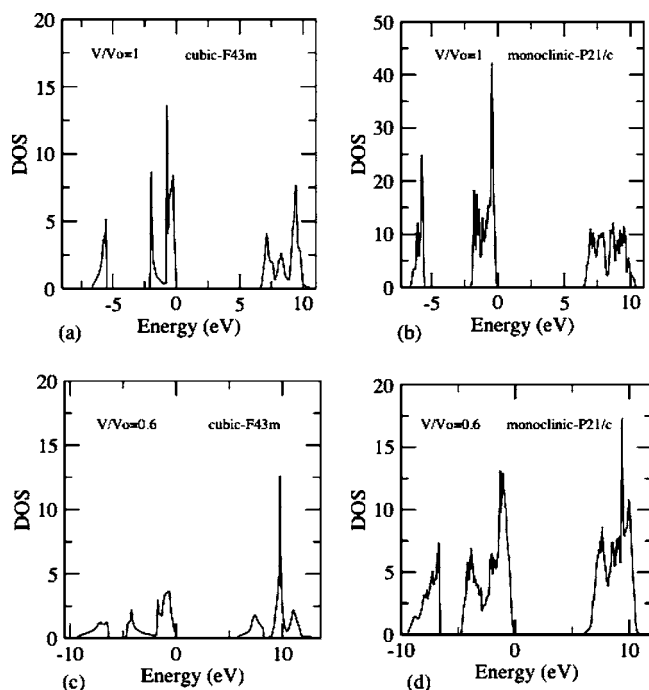
FIG. 9. Density of states for α-NaBH$_4$ phase (a) and (c) and for β-NaBH$_4$ phase (b) and (d). The Fermi level is set at zero energy.

ciated with the *shortening* of Na-nearest neighbors bond length. The low and high energy regions of the valence band have the same bandwidth as in α-NaBH$_4$. This is consistent with the slight change in the nearest B-H bond lengths.

Figures 9(c) and 9(d) show the correspondent DOS for the α- and β-NaBH$_4$ phases at a compressed volume V/V_0 $=0.6$, where the V_0 is the equilibrium volume for each phase. As one can observe, the bands become broader and the fundamental band gap tends to increase.

IV. CONCLUSIONS

In summary, we present a combined experimental and theoretical study of NaBH$_4$ under high pressure. Using Raman spectroscopic technique, we show that NaBH$_4$ undergoes a pressure-induced phase transition from its fcc structure to a new high-pressure phase. The transformation starts above 10 GPa with the pure high-pressure phase being established above 15 GPa, and it is shown to be reversible with respect to pressure release. A transition back to the α phase occurs at the somewhat lower pressures of 11–8 GPa. From the analysis of the Raman spectra, the new high-pressure phase is expected to be either orthorhombic or monoclinic, with the BH$_4$ cluster displaying lower symmetry. Through a cooling experiment, we also show that the new high pressure phase does not correspond to the low-temperature tetragonal (P -42_1c) phase. The theoretical investigation was performed within the framework of GGA to DFT using PAW method. We find that the new high-pressure phase corresponds to the α-LiAlH$_4$–type structure. The calculated transition pressure of 19 GPa agrees quite well with the experimental finding of 15 GPa. Furthermore, a slight distortion observed in the BH$_4$ supports the lower symmetry expected for this cluster. A subsequent phase transition is predicted to occur from β- to γ -NaBH$_4$ at 33 GPa. This is a prediction. We welcome new experiments to confirm this prediction. In addition, we also discuss the electronic structure of both α- and β-NaBH$_4$. The main change corresponds to the band gap narrowing in the β-NaBH$_4$, which is explained to be due to the broadening of Na antibonding states in the conduction band.

[1] L. Schlapbach and A. Züttel, Nature (London) **414**, 353 (2001).

[2] W. Grochala and P. P. Edwards, Chem. Rev. (Washington, D.C.) **104**, 1283 (2004).

[3] B. Bogdanovic and M. Schwickardi, J. Alloys Compd. **253**, 1 (1997).

[4] P. Vajeeston, P. Ravindran, R. Vidya, H. Fjellvåg, and A. Kjekshus, Appl. Phys. Lett. **82**, 2257 (2003).

[5] P. Vajeeston, P. Ravindran, R. Vidya, H. Fjellvåg, and A. Kjekshus, Phys. Rev. B **68**, 212101 (2003).

[6] A. V. Talyzin and B. Sundqvist, Phys. Rev. B **70**, 180101(R) (2004).

[7] Z. P. Li, N. Morigazaki, B. H. Liu, and S. Suda, J. Alloys Compd. **349**, 232 (2003).

[8] Z. P. Li, B. H. Liu, K. Arai, N. Morigazaki, and S. Suda, J. Alloys Compd. **356**, 469 (2003).

[9] Z. P. Li, B. H. Liu, K. Arai, K. Asaba, and S. Suda, J. Power Sources **126**, 28 (2004).

[10] C. Wu, H. Zhang, and B. Yi, Catal. Today **93**, 477 (2004).

[11] R. L. Davis and C. H. L. Kennards, J. Solid State Chem. **59**, 393 (1985).

[12] W. Kohn and L. J. Sham, Phys. Rev. **140**, A1133 (1965).

[13] P. E. Blöchl, Phys. Rev. B **50**, 17953 (1994).

[14] G. Kresse and J. Furthmüller, Phys. Rev. B **54**, 11169 (1996).

[15] J. P. Perdew and Y. Wang, Phys. Rev. B **45**, 13244 (1992).

[16] W. H. Press, B. P. Flannery, S. A. Teukolsky, and W. T. Vetterling, *Numerical Recepies* (Cambridge University Press, New York, 1986).

[17] P. E. Blöchl, O. Jepsen, and O. K. Andersen, Phys. Rev. B **49**, 16223 (1994).

[18] D. G. Allis and B. S. Hudson, Chem. Phys. Lett. **385**, 166 (2004).

[19] H. L. Johnston and N. C. Hallett, J. Am. Chem. Soc. **75**, 1467 (1953).

[20] W. H. Stockmeyer and C. C. Stephenson, J. Chem. Phys. **21**, 1311 (1953).

[21] B. Sundqvist, Adv. Phys. **48**, 1 (1999).

[22] K. Miwa, N. Ohba, S. I. Towata, Y. Nakamori, and S. I. Orimo, Phys. Rev. B **69**, 245120 (2004).